ISSN 0348-7539

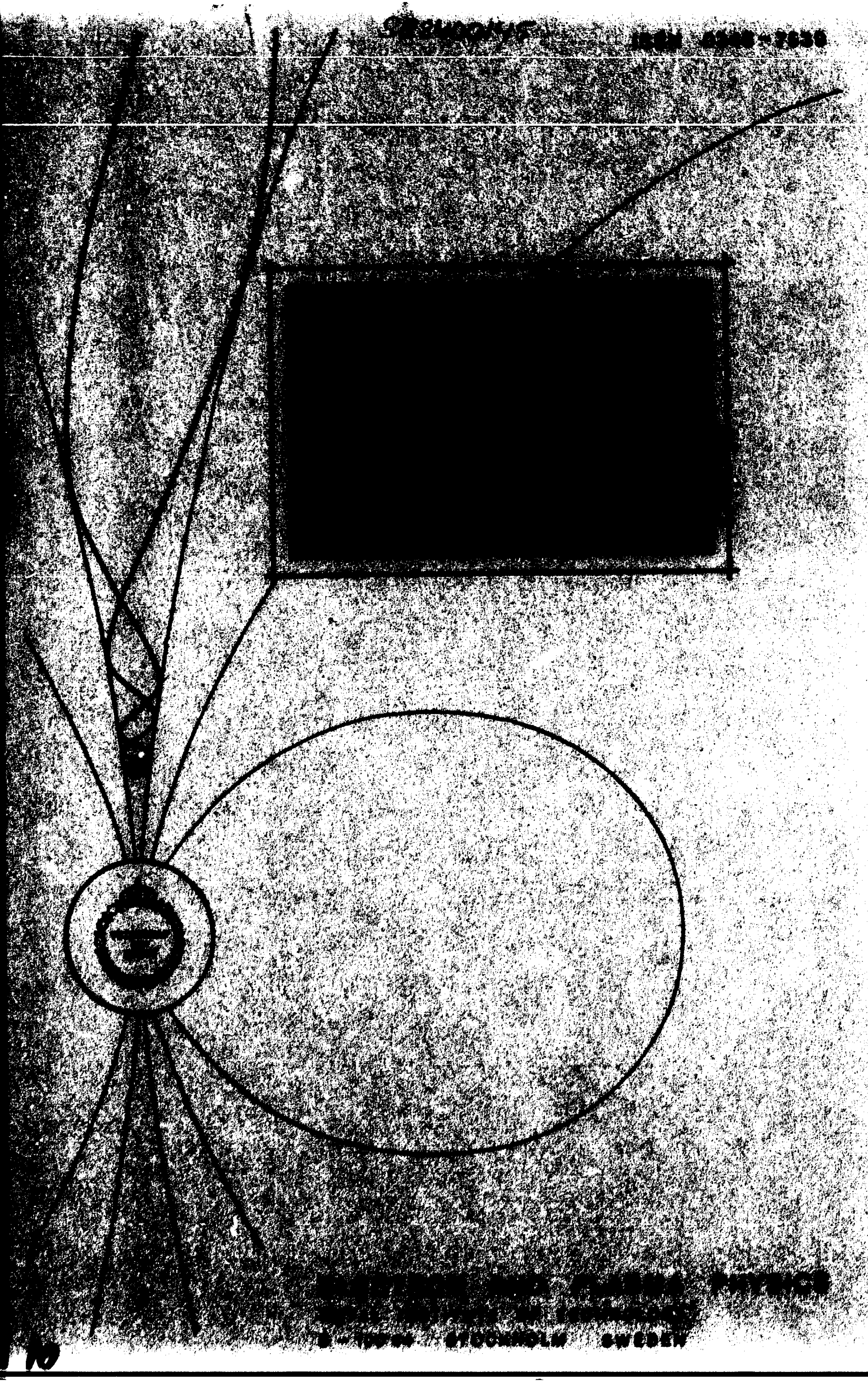

DEPARTMENT OF PLASMA PHYSICS
ROYAL INSTITUTE OF TECHNOLOGY
S-100 44 STOCKHOLM SWEDEN

10

TRITA-EPP-84-05

ROCKET AND SATELLITE OBSERVATIONS OF ELECTRIC FIELDS AND ION CONVECTION IN THE DAYSIDE AURORAL IONOSPHERE

G. Marklund and R.A. Heelis*

June 1984

Department of Plasma Physics
Royal Institute of Technology
S-100 44 Stockholm, Sweden

*Centre for Space Sciences, The University of Texas at Dallas,
P.O. Box 688, Richardson, TX 75080, USA

ROCKET AND SATELLITE OBSERVATIONS OF ELECTRIC FIELDS AND ION CONVECTION IN THE DAYSIDE AURORAL IONOSPHERE

G. Marklund(1) and R.A. Heelis(2)

Abstract

Electric field observations from two high-altitude rocket flights in the polar cusp have been combined with satellite observations of ion drifts to infer details of the electric field and convection pattern of the dayside auroral ionosphere. A region of shear flow reversal can be inferred from the electric field observations on one flight near 15.30 MLT 20 minutes after the Dynamics Explorer 2 satellite crossed through the same region. The drift patterns observed by the two spacecrafts were very similar although shifted by 0.5 degrees, a shift which is expected from the observed change in the interplanetary magnetic field (IMF) B_z component during this time. A region of rotational flow reversal was covered by the other flight shortly after magnetic noon, at the same time the DE-2 satellite travelled along roughly the dawn-dusk meridian. By joining points of equal potential, integrated from the two datasets and assuming the reversal boundary to be an equipotential, the instantaneous convection pattern could be drawn showing crescent-shaped convection contours in the dusk cell and more circular shaped contours in the dawn cell. In order to reproduce this pattern using the convection model recently proposed by Heelis <u>et al</u>. (1982) it was found necessary to introduce a local-time dependence of the decay of the electric field with distance from the reversal boundary. Moreover this pattern is shown to be qualitatively in agreement with the predictions of a geometrical model by Crooker (1979) when the IMF is oriented towards dawn. The same characteristic patterns but with the dusk and dawn cells reversed, as presented in a recent radar-satellite study for the IMF oriented towards dusk may serve as additional evidence in favour of this model.

(1) Dept of Plasma Physics. The Royal Institute of Technology, S-100 44 Stockholm, Sweden

(2) Centre for Space Sciences, The University of Texas at Dallas, P.O. Box 688, Richardson, TX 75080, USA

1. Introduction

The dayside auroral ionosphere and the polar cusp have attracted specific interest due to the fact that fundamental processes taking place in the outer magnetosphere, its boundary regions and the magnetosheath are reflected here and focused to a relatively small area easily accessible for observations by spacecraft and from the ground.

Electric fields have been measured in this region either directly by double probes on satellites (Cauffmann and Gurnett, 1972), rockets (Maynard et al., 1974; Ungstrup et al, 1975; Primdahl et al. 1979, 1984; Jorgensen et al, 1980; Kintner et al., 1978; Daly and and Whalen, 1978) and balloons (Mozer et al, 1974) or indirectly from the motion of Barium clouds (Wescott et al. 1978) or the ambient ion drift as observed by backscatter radars (Foster et al, 1981). Many of these studies suffer from an insufficient data coverage to enable an instantaneous picture of the large scale electric field or convection pattern to be constructed. In the vicinity of auroral arcs, arc-associated electric fields associated with Birkeland currents and polarisation electric fields may drastically change and complicate the picture (Marklund et al, 1983, 1984). Direct measurements of the plasma motion as observed by earth orbiting satellites (Hanson and Heelis, 1975) formed the starting point for more systematic studies of the large scale convection pattern. Not until recently was an attempt made to reconstruct the instantaneous convection pattern using simultaneous satellite (DE-2) and radar observations (Chatanika, Millstone Hill) for a number of events with the interplanetary magnetic field pointing towards dusk (Heelis et al, 1983). By joining points of equal potential integrated from the various datasets, instantaneous equipotential contours could be constructed showing a crescent-shaped and narrow dawn cell and a wider and circular-shaped dusk cell The only local time sector for which the data coverage was poor or missing was between 11.00 MLT and 16.00 MLT i.e. an important part of the dayside auroral oval.

In this study we have concentrated upon this region to enable a detailed picture of the dayside convection pattern close to the convection reversal boundary. Thus, a region of rotational flow reversal is covered by one rocket flight shortly after magnetic noon while the DE-2 satellite travelled in essentially the dawn dusk meridional plane. For this event detailed equipotential contours could be drawn based on the two datasets described in Section 4.

The other rocket passed through a region of shear flow reversal as inferred from electric field observations close to 15.30 MLT. Since the same region was passed within 20 minutes by the DE-2 satellite, the two datasets together provide very detailed information on the convection reversal itself but cannot be used to draw the instantaneous convection pattern as in the other case.

Additional plasmadrift observations are provided by the Sachs Harbour radar from a region close to the reversal boundary more towards noon than the rockets.

An important point is that the two events discussed here were geomagnetically quiet, with a relatively stable orientation of the IMF, as will be described in more detail in Section 3. This implies that any large temporal variations are not likely to have occured during the short time intervals between the different datasets.

2. Instrumentation

As part of the Project CENTAUR two Black Brant 10 rockets were launched from Cape Parry (invariant latitude 75°), Canada in December 1984, to study the electrodynamics of the polar cusp. The payloads carried detectors to measure the energetic particle composition, DC and AC electric and magnetic fields, plasma density and temperature and finally the ion drift. We shall here concentrate on the observations made by The Royal Institute of Technology (RIT) double probe electric field experiments on the two rockets. Observations of the other parameters mentioned above will be described in companion papers. The RIT experiment can be operated in two modes, the high impedance mode providing vector electric field measurements with a time resolution of 3 ms and the Langmuir mode providing information on plasma density and temperature every 5 s. A detailed description of the operational modes for a similar experiment is given in Marklund *et al* (1981). After subtraction of the $\underset{\sim}{v} \times \underset{\sim}{B}$ contribution the electric field has been transformed to a local geomagnetic coordinate system with the north axis oriented approximately 36^{o} clockwise from geographic north.

At the time of the two CENTAUR flights the DE-2 satellite crossed the high-latitude northern hemisphere along approximately the dawn-dusk meridian. During these passes, taking about 20 minutes between the 50^{o} invariant latitude on the dawn and dusk side, the ion drift velocity is measured every second along the satellite track. Only the component perpendicular to the trajectory is available for these two events. Details of this experiment and the DE-2 satellite have been given by Hoffmann (1981).

A number of ground-based experiments delivered important information on the geophysial conditions during the two events. These will be discussed in Section 3. The Sachs Harbour radar provided plasma irregularity drift observations as deduced from the received scattered signals originating from a satellite transmitter. Due to the geometry of the irregularities and the viewing direction of the radar only the drift component in roughly the geomagnetic north-south direction is available.

3. Geophysical conditions

Event 1: December 1, 1981

The CENTAUR 35.001 rocket was launched from Cape Parry at 01.38 UT (15.00 MLT) during a geomagnetically very quiet period as demonstrated by Fig. 1a, showing the magnetometer H-component from the Alaska meridian chain for a 24 hour period including the flight. The 3-hour K_p-index was 0+. In Fig. 2a the interplanetary magnetic field data are plotted as vectors in the x-y and y-z planes respectively. The vectors have been averaged over the time intervals indicated by the attached numbers, during which the IMF-orientation was relatively stable. A toward sector of the IMF with a strong sunward component (B_x>0), a somewhat weaker component towards dawn (B_y<0) and an even smaller z-component that changed from negative to positive about one and a half hour before launch, characterized this event.

Event 2: December 13, 1981

The CENTAUR 35.002 rocket was launched at 22.54 UT (12.30 MLT) on December 13, a day characterized by moderate geomagnetic activity as can be seen in Fig. 1b.

Several hours before launch, however, the activity dropped away almost completely. The 3 hour K_p-index during this flight was 1. The IMF data are plotted in Fig. 2b as vectors averaged over 15 minutes intervals starting at the indicated times before launch.

The two rockets were launched from Cape Parry (invariant latitude 75.^{o}) in a direction roughly towards local geomagnetic north. They reached an apogee of about 670 km 7.5 minutes after launch and traversed 7^o of invariant latitude. The spin axes of the rockets were kept closely parallel to the directions of the local magnetic field with an almost negligible coning angle.

A more comprehensive report on the project CENTAUR and the geophysical conditions and initial results will be given in a companion paper.

4. Observations

4.1 Rocket and radar observations

The result of the electric field data analysis for the two CENTAUR flights on December 1 (afternoon) and December 13 (noon) are plotted in Figs. 3a and 3b respectively. A similar trend can be recognized for the two events namely a reversal of the geomagnetic northward component while the eastward component is positive throughout the flight and shows less variation. Datagaps are seen in Fig 3a corresponding to periods for which the electric field probes were saturated and intense ion beams were observed. This will not be treated here but in a separate paper. In Figs. 4a and 4b 10 s averages of the data shown above are plotted as electric field vectors every half minute along the 100 km magnetic footpoint of the rocket trajectory. By comparing the reversals for the two events one notes the following:

1) The reversal for the afternoon event (Event 1) occured almost two degrees more poleward than for the noon event (Event 2).

2) The eastward component of the electric field tends to zero at the reversal boundary for the afternoon event thus indicating an equipotential boundary. This is not the case for the noon event.

3) Poleward of the reversal boundary an abrupt variation is seen in Fig. 3a in the northward electric field component. An almost 1:1 correspondence is found between this and the magnetic disturbance in the perpendicular direction as observed by the onboard magnetometers (data not shown here), reflecting a passage through adjacent field aligned

current sheets. This is treated in a separate paper (Primdahl _et al._, 1984).

4) The electric field was very intense during the noon event especially poleward of the reversal where it exceeds 100 mV/m, while it was weaker for the afternoon event.

In Fig. 5 the ExB/B^2 drifts as inferred from the electric field data for the two events are presented in an invariant-latitude vs magnetic local time diagram. A rotational reversal with relatively strong northward drifts can be recognized for the noon event and a shear flow reversal for the afternoon event that is an equivalent description of observation 2 above.

Figs. 6a and 6b show the northward component of the irregularity drifts, as observed by the Sachs Harbour radar, during the afternoon and noon events, respectively, in the vicinity of the convection reversal boundary. For the afternoon event, the northward drift was very small as expected for a shear flow reversal, while for the noon event the drift was considerably larger, consistent with a rotational flow reversal. A relativey good agreement can be seen between the rocket and radar observations in the region of closest approach between the two that is indicated by the shaded area.

In Fig. 7 are shown the electron density and temperature as deduced from the Langmuir sweeps of the RIT experiment on the noon flight. The electron density variation reflects an altitude variation with an F-region peak of about 5 10^{11} m^{-3}, seen close to 400 km altitude during the upleg. An increase in T_e from about $2000^{o}K$ to $3000^{o}K$ can be seen in the later part of the flight, within the polar cap. Corresponding data for flight 1 have not yet been evaluated.

DE-2 observations

In Fig. 8a the DE-2 perpendicular ion drifts are shown from a northern hemisphere crossing between 1.15 UT and 1.35 UT on December 1 shortly before the launch of the CENTAUR 35.001 rocket at 01.38 UT. A pronounced region of sunward convection on the duskside accompanied by somewhat more structured antisunward flow in the polar cap is seen. The division between plasma circulating around the dawnside and around the duskside marked by the location of a "zero potential" line occurs close to the noon midnight meridian and the maximum and minimum potentials of +8 kV and -15 kV observed by DE-2 occur at 82° and 79° invariant latitude, respectively. By comparing with the ExB/B^{2} drift vectors calculated for this flight, as shown in Fig. 5, one notes that the rocket and satellite trajectories almost overlap close to the the dusk reversal boundary, and that its location agrees well between the two datasets. This is more clearly seen in Fig. 9, showing the DE-data together with the sunward component of the CENTAUR driftvectors, which have been projected to DE trajectory along circles of constant invariant latitude. Note that the observed drift patterns are very similar although a poleward shift of 0.5 to 1 degree can be recognized during the twenty minute interval between the DE and the CENTAUR observations. Such a shift is consistent with a shrinking polar cap that might be expected for the observed change in the IMF B_z-component from south to north, taking place roughly one hour before the rocket launch. Relatively small drift velocities prevailed along the entire dawn-dusk meridian during this flight.

In Fig. 8b the perpendicular ion drifts are shown for a DE-2 crossing between 22.25UT and 22.45 UT on December 13, shortly before launch of the CENTAUR 35.002 rocket at 22.54 UT. A two-cell convection pattern of a more common form can be recognized for this event with antisunward flow in almost the entire polar cap region between invariant latitude 75° and 76° on the dawn and dusk side respectively. The flow velocities were obviously larger for this event, increasing from the dawn to the dusk side.

Due to the good data coverage by the rocket close to magnetic noon and by the DE-2 satellite in roughly the dawn-dusk meridional plane, separated in time by less than 30 minutes, a detailed picture of the dayside convection pattern can be inferred. In Fig. 10a the high-latitude region above invariant latitude 70^{o} from Fig. 8b has been enlarged and supplemented in the following way: Points of equal potential integrated from the rocket and satellite data along their respective trajectories have been joined under the assumption that the convection reversal boundary is almost an equipotential; and with the requirement that the drift vectors are tangential to the equipotential surfaces. The latter requirement can be used only on the rocket data since the longitudinal component of the DE-2 drifts is missing. Thus, there is still some uncertainty about the exact orientation of the equipotential surfaces along the satellite path although they are accurately located. It can be seen that the dayside pattern is characterized by crescent-shaped convection contours in the dusk cell compressed towards noon with a reversal boundary potential of about -37 kV and a potential distribution in the dawncell indicative of an anticlockwise circularshaped flow pattern with a reversal boundary potential of about 13 kV. Assuming the convection reversal boundary forms a circle passing through the dawn and dusk reversals at invariant latitude 76.^{o}5 and 75^{o} respectively given by the DE-2 data and the rotational reversal at 77.^{o}2 close to noon given by the rocket data, the polar cap radius becomes about 14.6^{o} with a centre shift of 2^{o} towards magnetic midnight. A more detailed picture of the dusk cell is shown in Fig. 10b.

5. Discussion

The high-latitude convection pattern is known to respond sensitively to variations in the interplanetary magnetic field. Any fruitful attempt to picture the instantaneous large scale convection pattern requires geophysically stable conditions over a period which exceeds both the typical response times for changes in the IMF and the data-taking periods. Since these times are typically 30 min. here and since it was geomagnetically quiet for several hours prior to launch (cf. Figs. 1a and 1b) and the IMF was stable for more than one hour (cf. Figs. 2a and 2b) for both events the above requirement was reasonably well fulfilled.

For both events the IMF B_y-component was negative (cf. Figs. 2a and 2b). When the IMF B_z-component is negative the above condition is known to produce an asymmetry in the convection pattern such that electric field maxima occur on the dusk side of the northern polar cap and the dawn side of the southern polar cap, as shown by e.g. Heppner (1972) and Mozer (1974). This asymmetry is clearly evident in Fig. 8b or Fig. 10a showing an increase in the drift velocities from the dawn to the dusk side. The maximum potential on the dusk side was -15 kV for the December 1 event and -37 kV for the December 13 event and the corresponding values on the dawn side were +8 kV and +13 kV, inferred from the integration of the DE-2 data.

The enhanced electron temperature of 3000°K observed by the rocket within the polar cap (cf. Fig. 7) may be related to the intense electric fields reaching 100 mV/m and corresponding intense drifts within this region.

For the December 1 event, good agreement between the rocket and satellite measurements of **E** x **B** drift is obtained in the duskside auroral zone. The characterization of a global convection pattern is made difficult by the northward IMF conditions prevailing for this event and by the fact that the rocket and satellite data were taken in about the same location. Several features are worthy of note. The convection signatures are generally consistent with two convection cells with sunward convection in the auroral zones both on the dawnside and the duskside. In the polar cap, identified by the absence of plasmasheet electrons observed on DE-2, the convection is extremely structured but has a small antisunward component.

For the December 13 event a much clearer and more easily characterized signature of the convection pattern is seen. This is possibly due to the fact that the IMF was here almost entirely directed toward dawn. In this pass the two convection cells appear to occupy about the same area on the dayside but crescent-shaped flow contours exist only for the higher negative potentials on the duskside. We note that at least some of the rotational reversal region seen by the rocket exists on the duskside of local noon.

The general flow patterns may be understood in terms of a geometrical model by Crooker (1979). Fig. 11 is a reproduction of Fig. 5 in this paper showing predicted polar cap convection patterns for various orientations of IMF in the y-z plane, attributable to merging of antiparallel field lines.

The predicted pattern for the December 1 event involves only one cell circulating completely within the polar cap. We cannot of course rule out such a possibility since the convection velocities involved may be small and extremely structured. Nevertheless, the most prominent features include two convection cells that include sunward convection in the dawn and dusk auroral zones. The electrostatic potentials associated with these cells are quite small and could be attributable to additional viscous interaction processes operating at the magnetopause (Crooker, 1977).

For the event of December 13 the predicted and observed convection patterns are more consistent. The crescent-shaped convection contours on the duskside are consistent with both dayside merging and viscous interaction, and we have not distinguished the relative importance of these mechanisms. On the dawnside the transition from sunward to antisunward flow is very structured and some small regions of sunward flow may exist within the polar cap as required by the model. It appears, however, that most of the flow is attributable to dayside merging even in this rather extreme orientation of the IMF.

In a similar study Heelis et al. (1983) present, on basis of radar and satellite observations, instantaneous pictures of the convection patterns for six events when the IMF B_y-component instead was positive. As expected the characteristic shapes of the dawn and dusk cells were reversed fitting qualitatively with the predicted patterns shown in Fig. 11 for various positive IMF B_y-orientations. The multiple observations covered essentially the entire nightside from local morning to local evening but not the afternoon sector on which we have concentrated in the present study.

To summarize, there is strong evidence in favour of the geometrical model by Crooker (1979), both from the dayside convection patterns observed in this study for IMF $B_y < 0$ and from the satellite-radar study by Heelis et al. (1983) for IMF $B_y > 0$.

An attempt was also made to reproduce the instantaneous dayside pattern drawn in Fig. 10 by fitting the model parameters in the convection model by Heelis et al. (1982). It was then found necessary to introduce some modifications in the model. For example, the dusk cell is, according to Fig. 10, more compressed close to magnetic noon than it is at dusk, especially poleward of the reversal boundary. By introducing a local time dependence for the electric field decay index describing how rapidly the field decays away from the reversal boundary this could be accounted for. An exponential increase in the decay index r_2 from about 2 at dusk to 5 at noon was found to reasonably well reproduce the observed pattern.

7. Conclusions

In this study a combination of electric field observations on two CENTAUR rocket flights in the polar cusp, ion drift observations on the DE-2 satellite along the dawn-dusk meridional plane and irregularity drift observations from the Sachs Harbour radar have been used to infer details of the electric field and the convection pattern of the dayside auroral ionosphere, during two geomagnetically quiet events when the IMF B_y-component was negative. The results can be summarized as follows.

1. On December 1, the same region, with a shear flow reversal, was traversed first by the DE-2 satellite and twenty minutes later by the 35.001 rocket. The drift patterns observed by the two spacecrafts were very similar although shifted by 0.5 degrees, a shift which is expected from the previously observed change in the IMF B_z-component. Additional evidence that the reversal is of the shear type and not the rotational type is given from simultaneous radar observations of almost negligible northward drifts at the reversal boundary.

2. On December 13, a region with a rotational flow reversal centered around $77.^{o}5$ was traversed by the 35.002 rocket close to magnetic noon, as the DE-2 satellite passed over the dawn and dusk reversal boundaries at 05.30 MLT and 16.30 MLT respectively. Intense northward drifts as observed by the Sachs Harbour radar at the reversal boundary serve as additional evidence that the reversal is of the rotational type. A detailed picture of the instantaneous dayside convection pattern could be drawn by joining points of equal potential integrated from the rocket and satellite data. The result shows a crescent-shaped dusk cell convection contours compressed towards noon and a more circular shaped dawn cell.

3. This detailed dayside pattern for the December 13 event and that inferred qualitatively for the December 1 event are shown to be generally consistent with those predicted from a geometrical model by Crooker (1979) for the given IMF-orientations with B_y negative. The addition of convective flow from a viscous interaction type mechanism is required when the IMF has a northward component. The same characteristic shapes but with the dusk and dawn cells reversed, as presented in a recent radar-satellite study for $B_y > 0$, may serve as additional evidence in favour of

this model.

4. In order to reproduce the dayside convection pattern presented above using the convection model by Heelis et al. (1983) it was found necessary to introduce a local-time dependent electric field decay index increasing exponentially towards noon.

Acknowledgements

The authors thank R. Mehra for part of the data analysis of the rocket data, L. Block, C.-G. Fälthammar and D.W. Winningham for helpful comments, S.-I. Akasofu for providing ground magnetometer data and J.A. McDougall for the Sachs Harbour radar observations, K. Forsberg for making the excellent drawings and E. Florman for typing the manuscript. This research was supported by the Swedish Board of Space Activities and by NASA grant NAG 5-306 and Air Force Geophysics Laboratory grant F19628-83-K-0022 to UTD.

References

Cauffman, D.P. and Gurnett, D.A., Satellite Measurements of High-Latitude Convection Electric Fields, Space Sci. Rev., 13, 369, 1972.

Crooker, N.U., The Magnetospheric Boundary Layers; A Geometrically Explicit Model, J. Geophys. Res., 82, 3629, 1977.

Crooker, N.U., Dayside Merging and Cusp Geometry, J. Geophys. Res., 84, 951, 1979.

Daly, P.W. and Whalen, B.A., Rocket-Borne Measurements of Particles and Ion Convection in Dayside Aurora, J. Geophys. Res., 83, 2195, 1978.

Foster, J.C., Doupnik, J.R. and Stiles, G.S., Ionospheric Convection and Currents in the Midnight Sector on Nov. 8, 1979, J. Geophys. Res., 86, 2217, 1981.

Hanson, W.B. and Heelis, R.A., Techniques for Measuring Bulk Gas Motions from Satellites, Space Sci. Instrum., 1, 493, 1975.

Heppner, J.P., Polar-Cap Electric Field Distributions related to the Interplanetary Magnetic Field Direction, J. Geophys. Res., 77, 4877, 1972.

Heelis, R.A., Lowell, J.K. and Spiro, R.W., A Model of the High-Latitude Ionospheric Convection, J. Geophys. Res., 87, 6339, 1982.

Heelis, R.A., Foster, J.C., de la Beaujardière, O. and Holt, J., Multistation Measurements of High-Latitude Ionospheric Convection, J. Geophys. Res., 88, 10111, 1983.

Hoffmann, R.A., Dynamics Explorer, Space Sci. Instrum., 5, 1981.

Jørgensen, T.S., Mikkelsen, I.S., Lassen, K., Haerendel, G., Rieger, E., Valenzuela, A., Mozer, F.S., Temerin, M., Holback, B. and Björn, L., Electric Fields in the Dayside Auroral Oval, J. Geophys. Res., 85, 2891, 1980.

Kintner, P.M.. Ackerson, K.L., Gurnett, D.A. and Frank, L.A., Correlated Electric Field and Low-Energy Electron Measurements in the Low-Altitude Polar Cusp, J. Geophys. Res., 83, 163, 1978.

Marklund, G., Block, L. and Lindqvist, P.-A., Rocket Measurements of Electric Fields, Electron Density and Temperature During Different Phasis of Auroral Substorms, Planet. Space Sci., 29, 249, 1981.

Marklund, G., Baumjohann, W. and Sandahl, I., Rocket and Ground-Based Study of an Auroral Breakup Event, Planet. Space Sci., 31, 207, 1983.

Marklund, G., Auroral Arc Classification Scheme Based on the Observed Arc-Associated Electric Field Pattern, Planet. Space Sci., 32, 193, 1984.

Maynard, N.C. and Johnstone, A.D., High-Latitude Dayside Electric Field and Particle Measurements, J. Geophys. Res., 79, 3111, 1974.

Mozer, F.S., Gonzalez, W.D., Bogott, F., Kelley, M.C. and Schutz, S., High-Latitude Electric Fields and the Three-Dimensional Interaction Between the Interplanetary and Terrestrial Magnetic Fields, J. Geophys. Res., 79, 56, 1974.

Primdahl, F., Walker, J.K., Spangslev, F., Olesen, J.K., Fahleson, U. and Ungstrup, E., Sunlit Cleft and Polar Cap Ionospheric Currents Determined from Rocket-Borne Magnetic Field, Plasma and Electric Field Observations, J. Geophys. Res., 84, 6458, 1979.

Primdahl, F., Bahnsen, A., Ejiri, M., Høeg, P., Marklund, G., Maehlum, B.N., Olesen, J.K., Ungstrup, E. and Zanetti, L.J., Rocket-Borne and Ground-Based Observations of Coincident Field-Aligned Currents, Electron Beams, and Plasma Enhancements in the Afternoon Auroral Oval, Planet Space Sci., 32, 561, 1984.

Ungstrup, E., Bahnsen, A., Olesen, J.K., Primdahl, F., Spangslev, F., Heikkila, W.J., Klumpar, D.M., Winningham, J.D., Fahleson, U., Fälthammar, C.-G. and Pedersen, A., Rocket-Borne Particle, Field and Plasma Observations in the Cleft Region, Geophys. Res. Lett., 2, 345, 1975.

Wescott, E.M., Stenbaek-Nielsen, H.C., Davis, T.N., Jeffries, R.A. and Roach, W.H., The Tordo 1 Polar Cusp Barium Plasma Injection Experiment, J. Geophys. Res., 83, 1565, 1978.

Figure captions

Fig.1 H-component of the ground magnetic disturbance as measured by the Alaska meridian chain of magnetometers during a) the Dec. 1 event and b) the Dec. 13 event. The shaded areas represent the flight periods.

Fig.2 Projections to the y-z and x-y planes of the interplanetary magnetic field as derived from ISEE-3 during a) the Dec. 1 event and b) the Dec. 13 event.

Fig.3 Horizontal electric field components vs flight time (s), altitude (km) and universal time in a coordinate system with local geomagnetic north 36° clockwise of geographic north. Derived from the RIT experiment on a) CENTAUR 35.001 on Dec. 1 and b) CENTAUR 35.002 on Dec. 13.

Fig.4 Vector representation of the results presented in Fig. 3 along the 100 km magnetic footpoint of the rocket a) 35.001 on Dec. 1 and b) 35.002 on Dec. 13.

Fig.5 $\underset{\sim}{E} \times \underset{\sim}{B}/B^2$ drifts corresponding to the electric field observations presented in Figs. 3 and 4 plotted in an invariant latitude vs magnetic local time diagram.

Fig.6 Geomagnetic northward component of the irregularity drift as measured by the Sachs Harbour radar during a) the Dec. 1 event and b) the Dec. 13 event. For comparison the corresponding drift component calculated from the rocket electric field data has been included.

Fig.7 Electron temperature and electron density vs flight time, altitude and universal time as deduced from the RIT Langmuir sweeps on flight 35.002, Dec. 13.

Fig.8 The perpendicular ion drift velocity measured by the DE-2 satellite a) between 01.15 and 01.35 UT on Dec. 1 and b) between 22.25 and 22.45 UT on Dec. 13. Also indicated are the potential distributions along the respective trajectories, as integrated from the DE-2 data.

Fig.9 Comparison of the sunward drift component observed on DE-2 and CENTAUR 35.001 in the dusk hemisphere around 01.40 UT on Dec. 1, 1981. For explanation, see text.

Fig.10a An instantaneous picture of the dayside convection pattern as inferred from the integrated CENTAUR electric field and DE-2 ion drift observations around 23.00 UT on Dec. 13, 1984. The estimated polar cap location is also indicated in the figure.

Fig.10b A detailed picture of the convection contours in the dusk cell, presented in Fig. 10a.

Fig.11 Reproduction of Fig. 5 in a paper by Crooker (1979) showing predicted polar cap convection patterns in the dayside northern hemisphere, viewed from above, for various orientations of the interplanetary magnetic field (IMF) in the y-z plane, attributable to merging of antiparallel field lines. The shaded regions are convection gaps. The IMF-orientation during the two events discussed here are also inserted in the figure.

ALASKA CHAIN OF MAGNETOMETERS, H TRACE

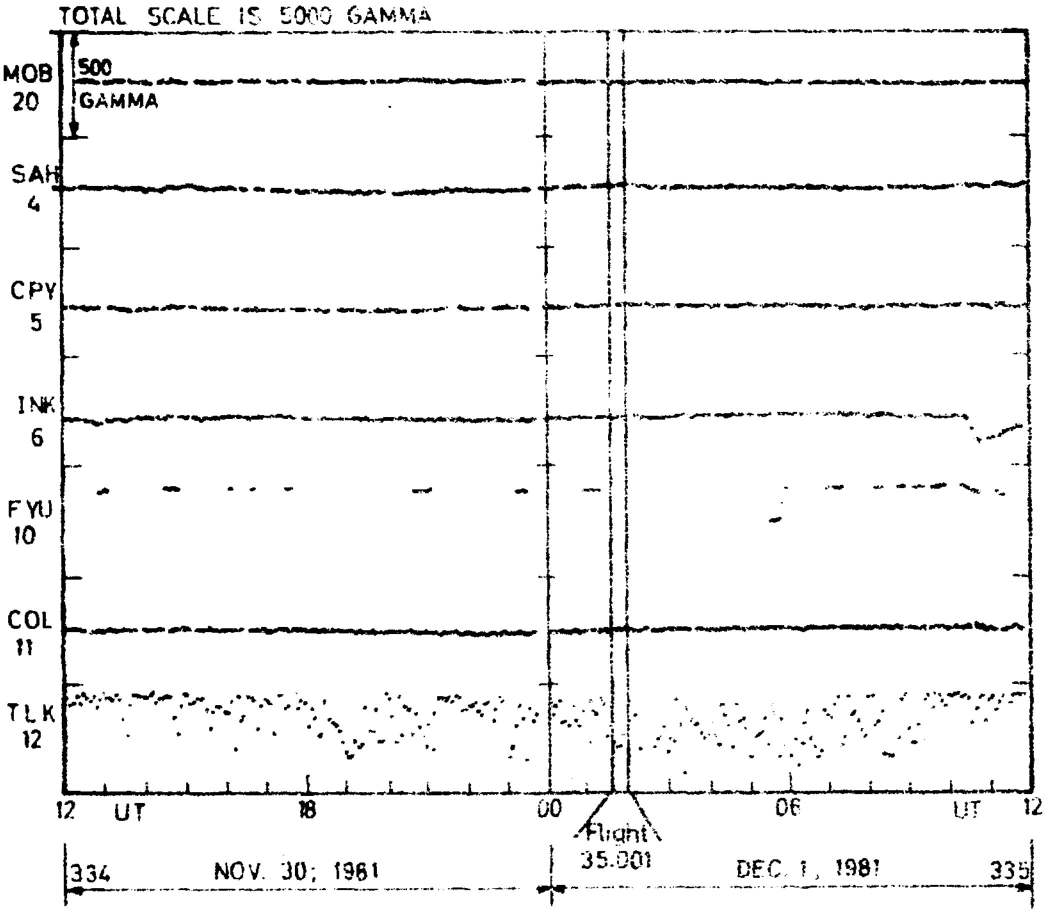

Fig. 1a

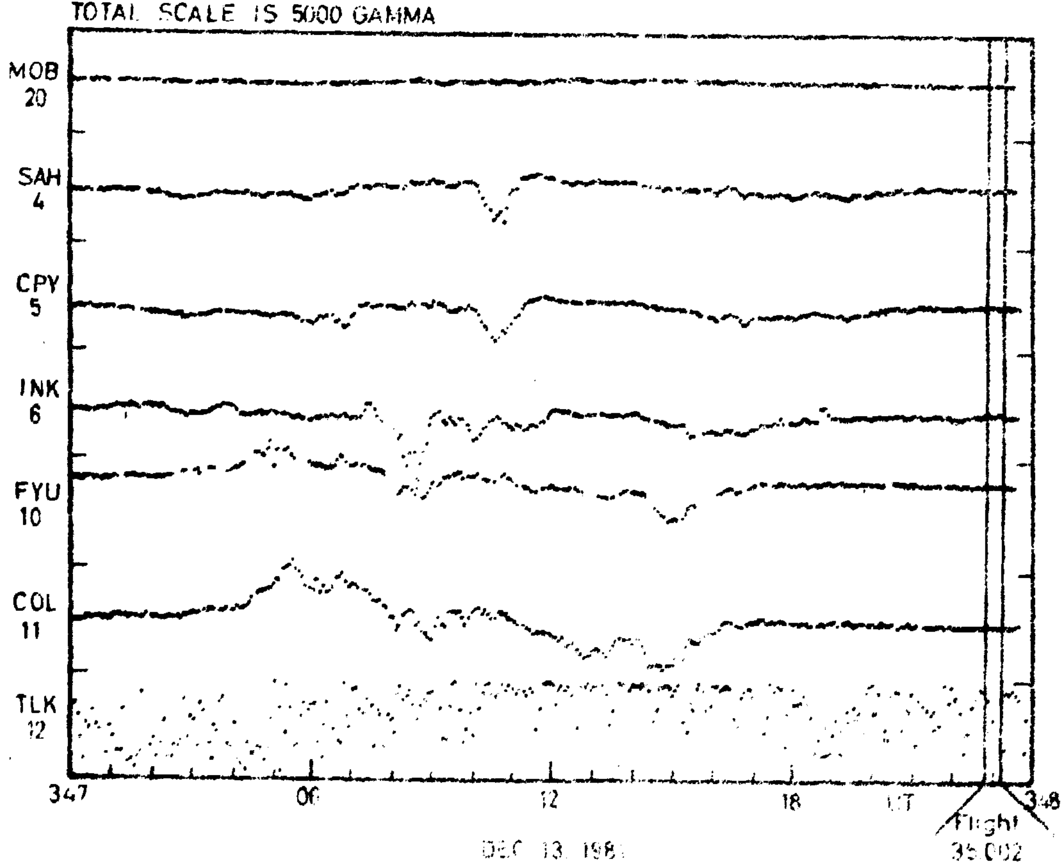

Fig. 1b

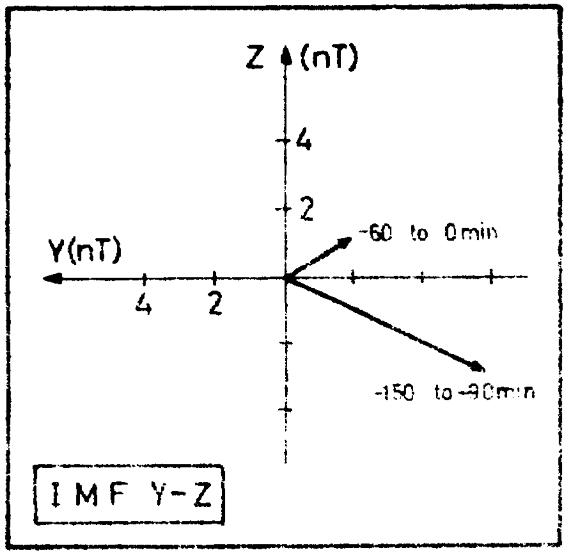

CENTAUR 35.001
23.00 UT nov. 30-02.00 UT dec 1, 1981

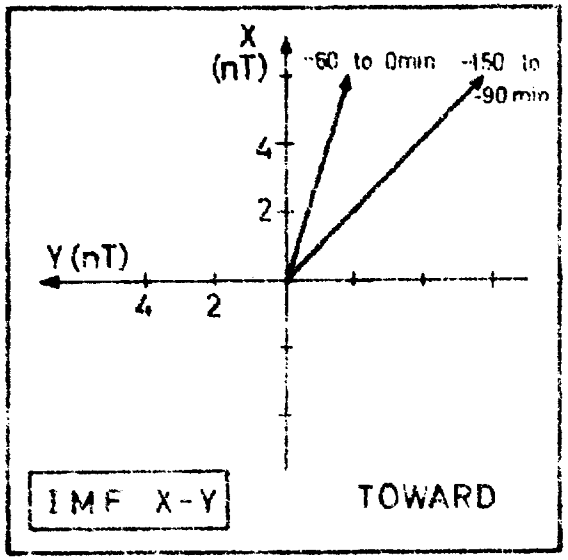

Fig. 2a

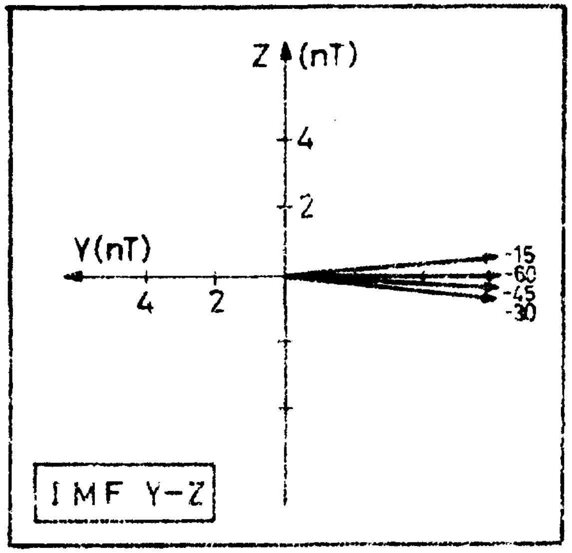

CENTAUR 35.002
21.55 UT-22.55 UT dec. 13, 1981

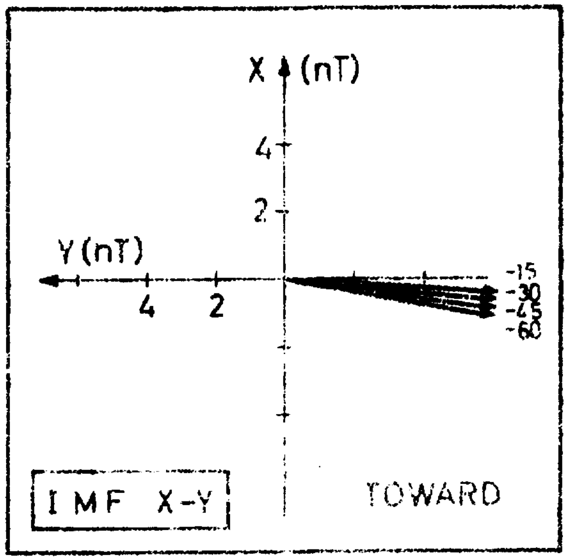

Fig. 2b

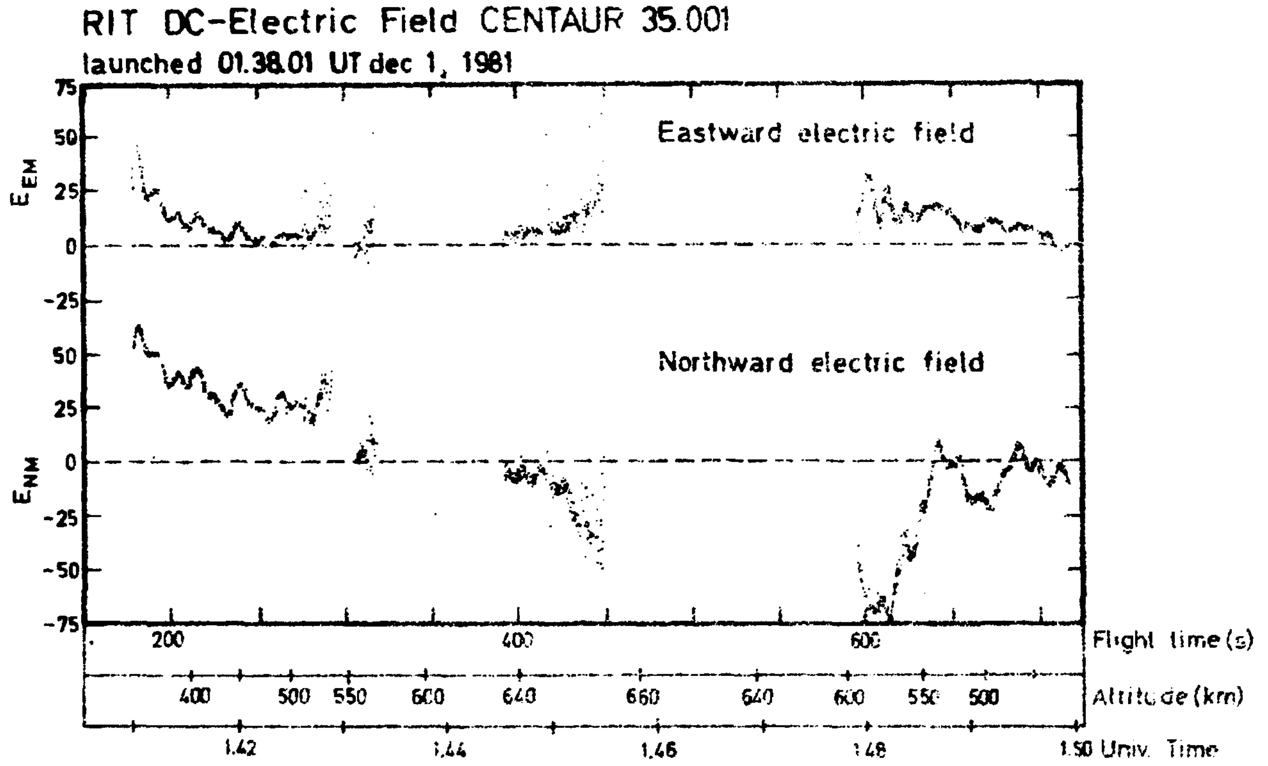
RIT DC-Electric Field CENTAUR 35.001
launched 01.38.01 UT dec 1, 1981
Eastward electric field
Northward electric field
E_{EM}
E_{NM}
75
50
25
0
-25
50
25
0
-25
-50
-75
200
400
600
Flight time (s)
400
500
550
600
640
660
640
600
550
500
Altitude (km)
1.42
1.44
1.46
1.48
1.50 Univ. Time

Fig. 3a

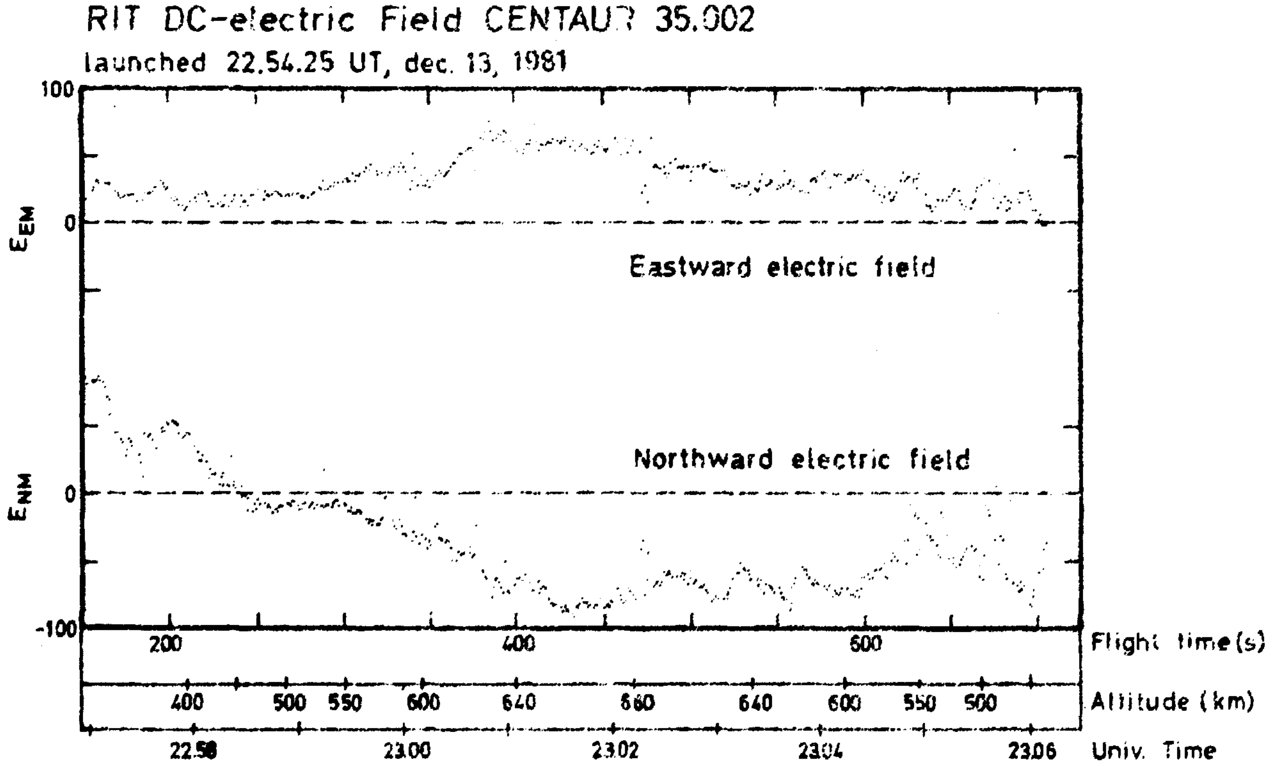
RIT DC-electric Field CENTAUR 35.002
launched 22.54.25 UT, dec. 13, 1981
Eastward electric field
Northward electric field
E_{EM}
E_{NM}
100
0
0
-100
200
400
600
Flight time (s)
400
500
550
600
640
660
640
600
550
500
Altitude (km)
22.58
23.00
23.02
23.04
23.06
Univ. Time

Fig. 3b

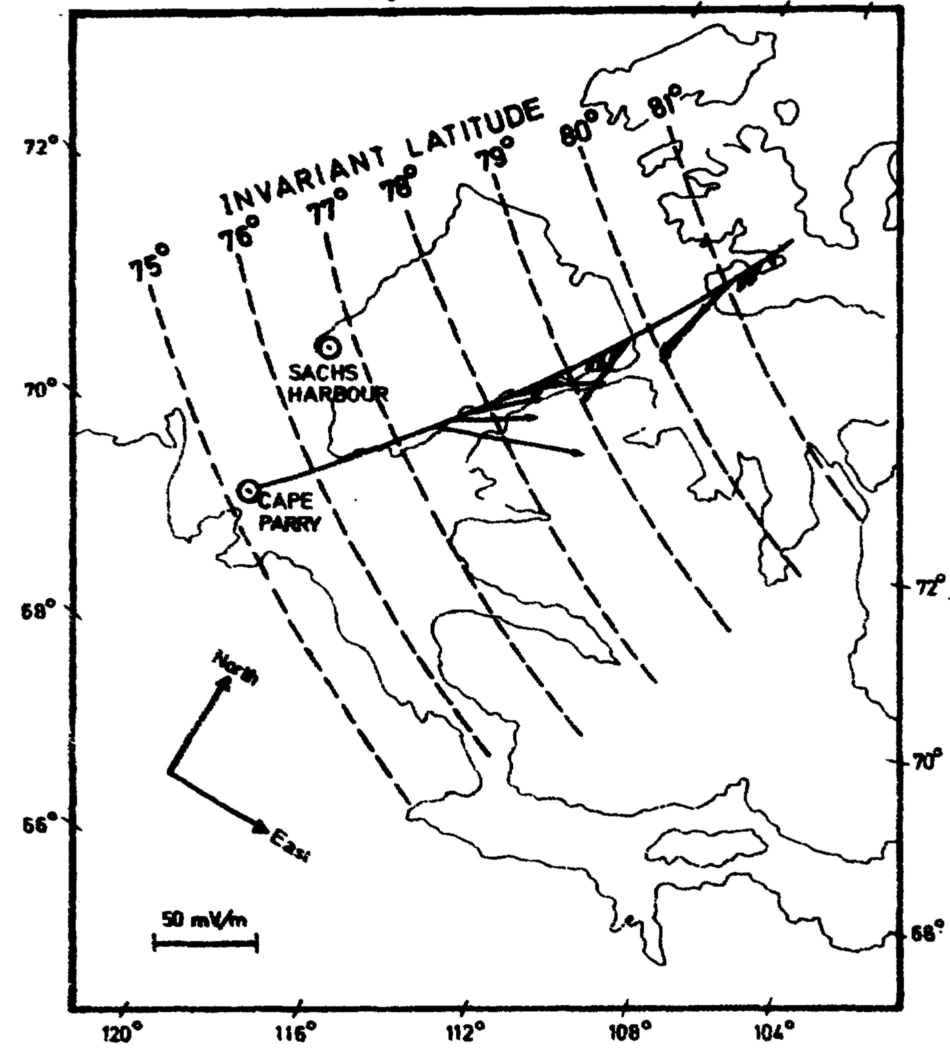

DC Electric field, CENTAUR 35.001

Launched 01.38.01 UT, Dec. 1 1981.

Fig. 4a

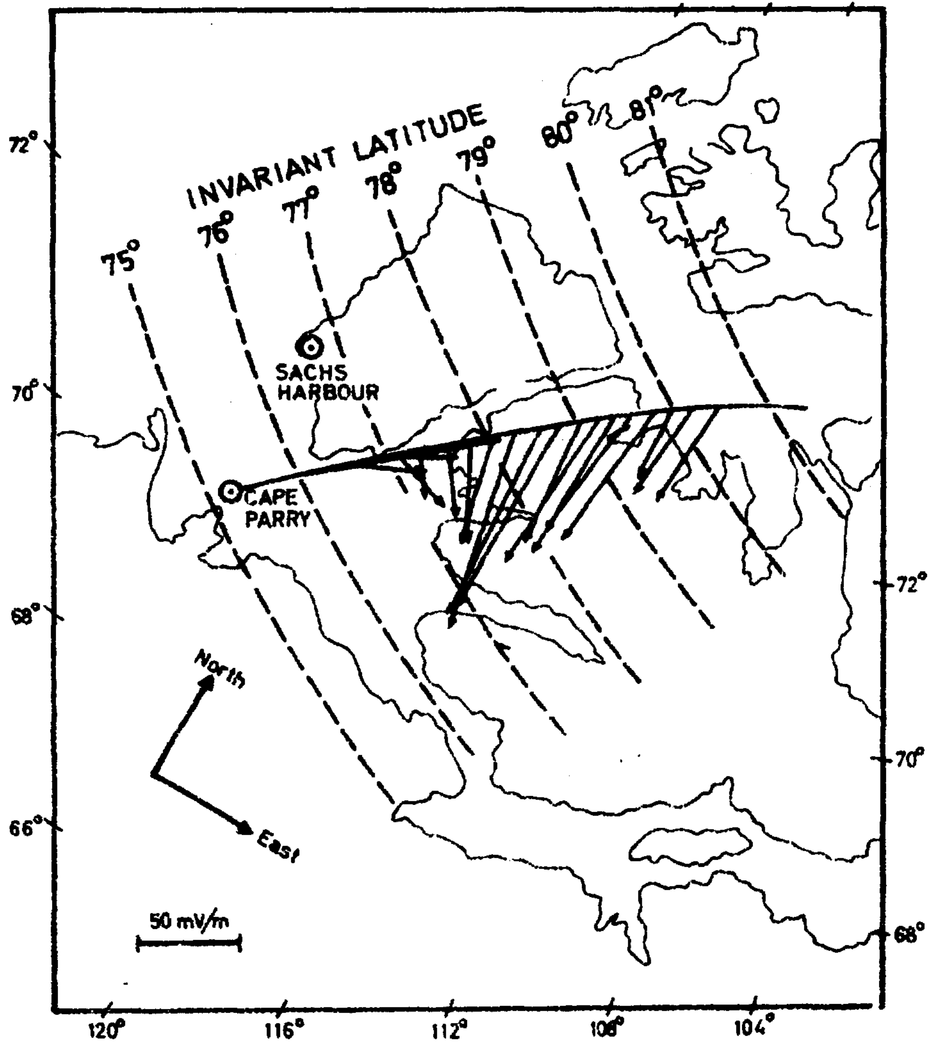

DC-Electric field, CENTAUR 35.002

Launched 22.54.25 UT, Dec. 13 1981.

Fig. 4b

$E \times B/B^2$ drifts calculated from the RIT DC electric field observations on CENTAUR flights 35.001 (01.38 UT, dec. 1) and 35.002 (22.54 UT, dec. 13).

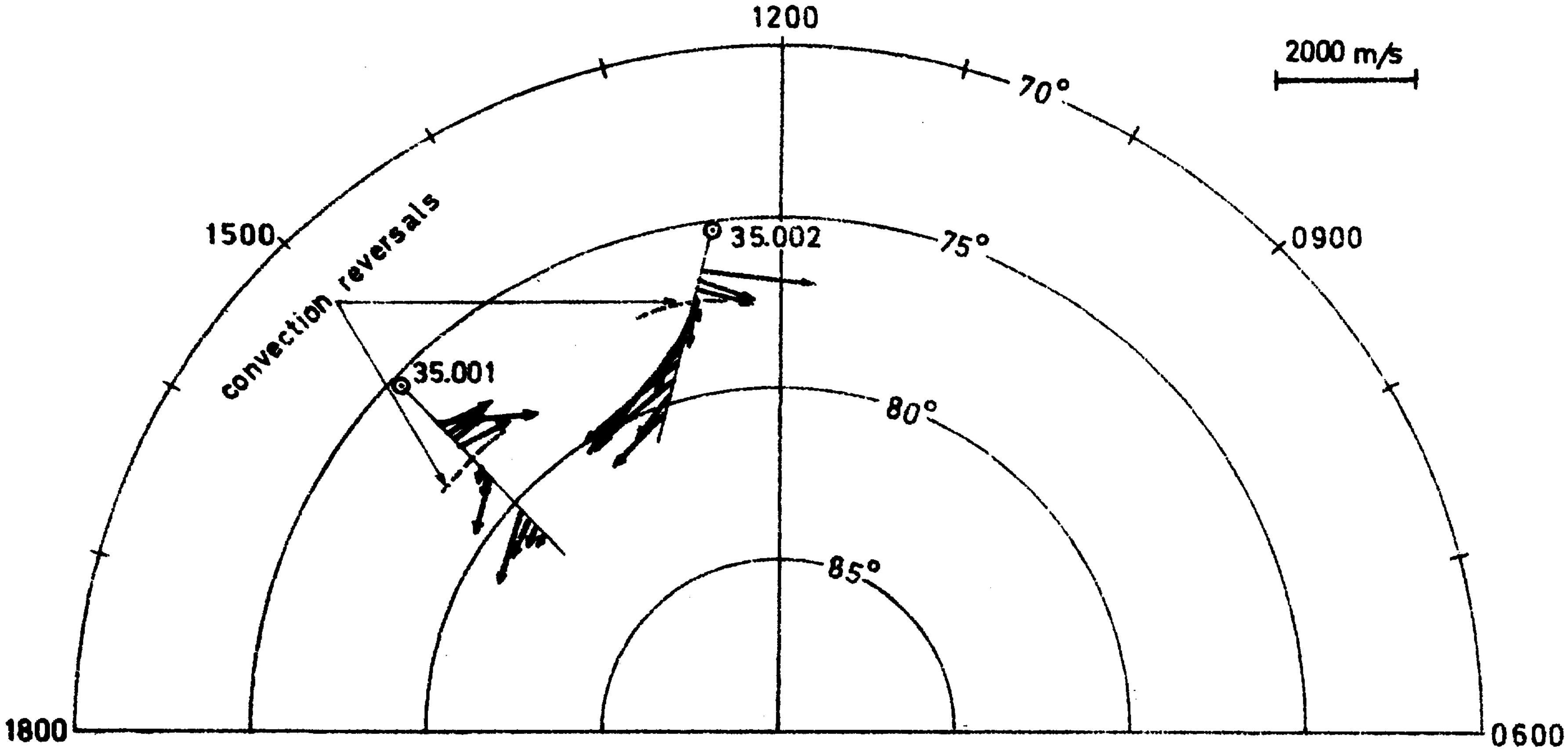

INVARIANT LATITUDE VS MAGNETIC LOCAL TIME

Fig. 5

ROCKET-RADAR COMPARISON OF NORTHWARD DRIFT COMPONENT

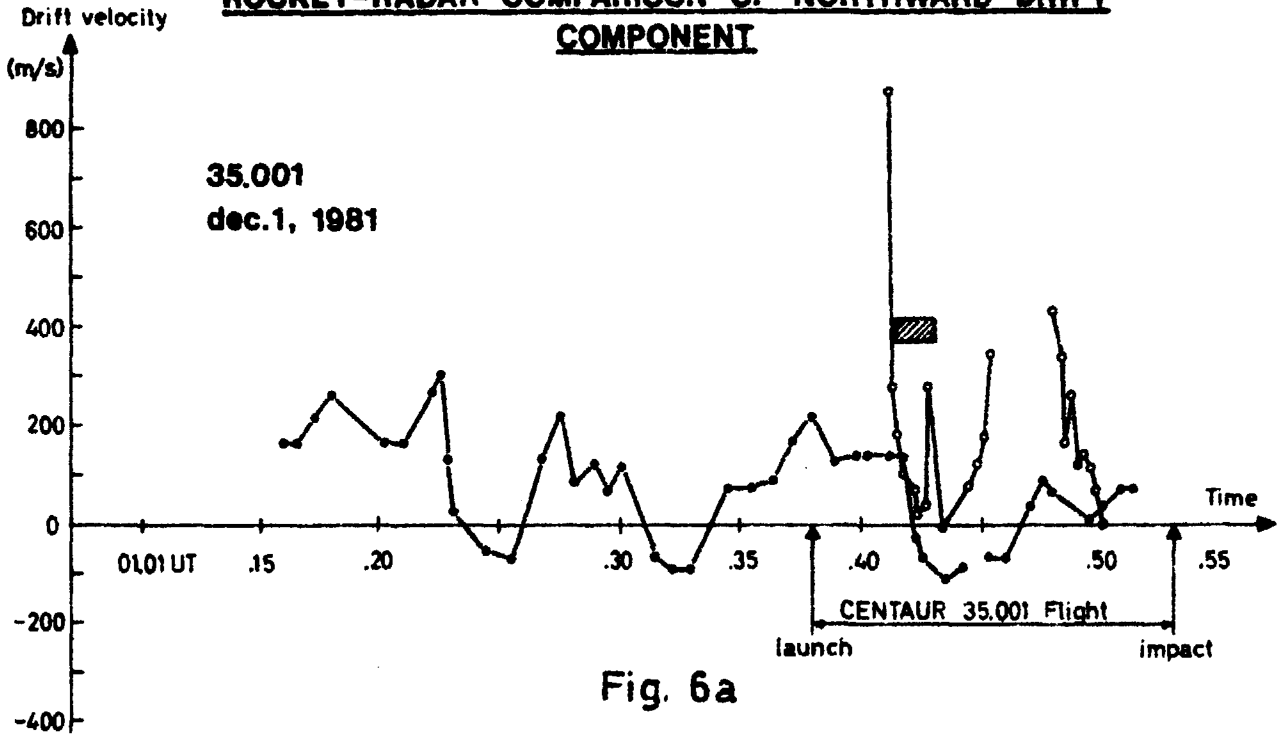

Fig. 6a

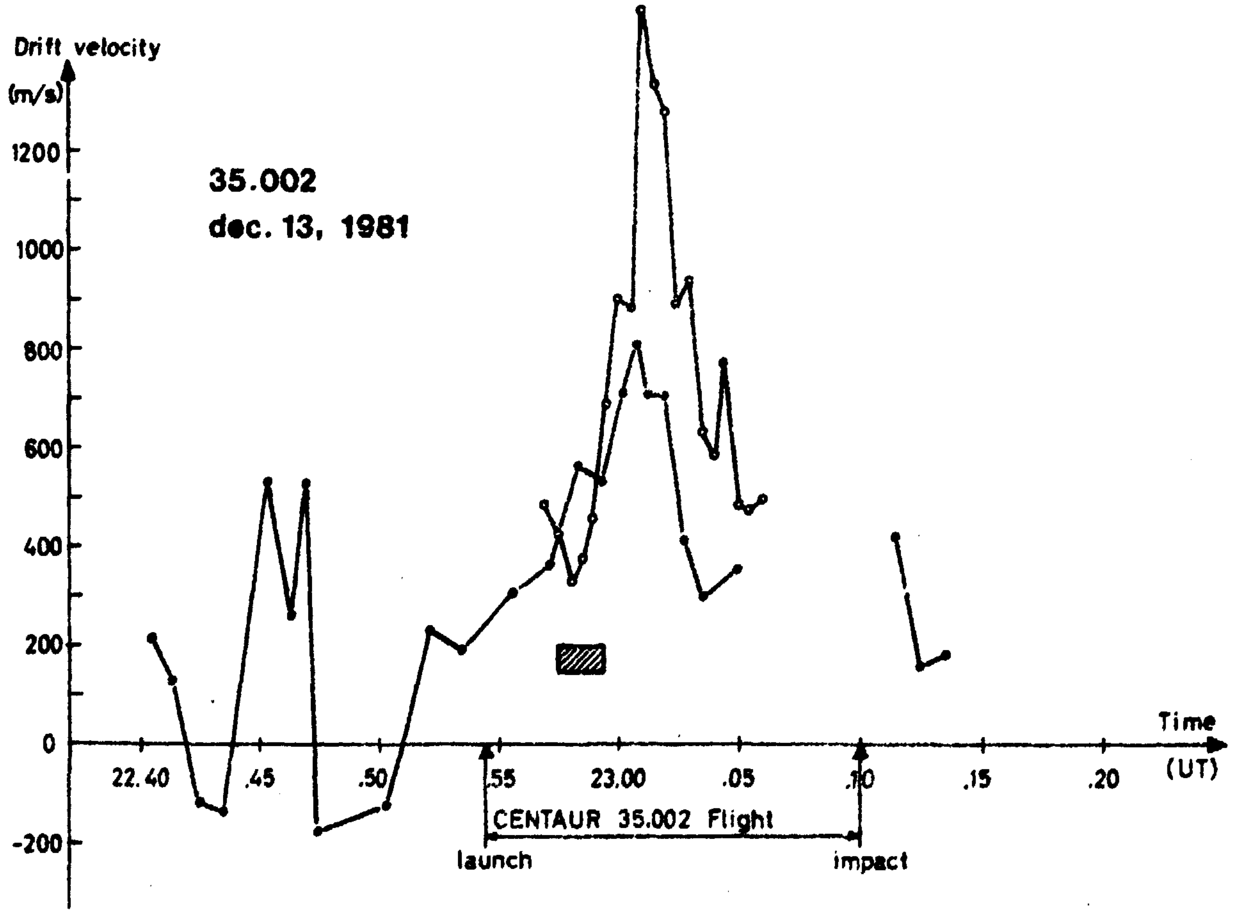

—•—•— N-ward irregular drift as observed by Sachs Harbour radar.

—○—○— N-ward $E \times B/B^2$ drift as calculated from CENTAUR electric field.

▨ Periods of closest approach and same invariant latitude between the two datasets.

Fig. 6b

RIT Plasma parameters. CENTAUR 35.002
launched 22.54.25 UT, dec., 1981

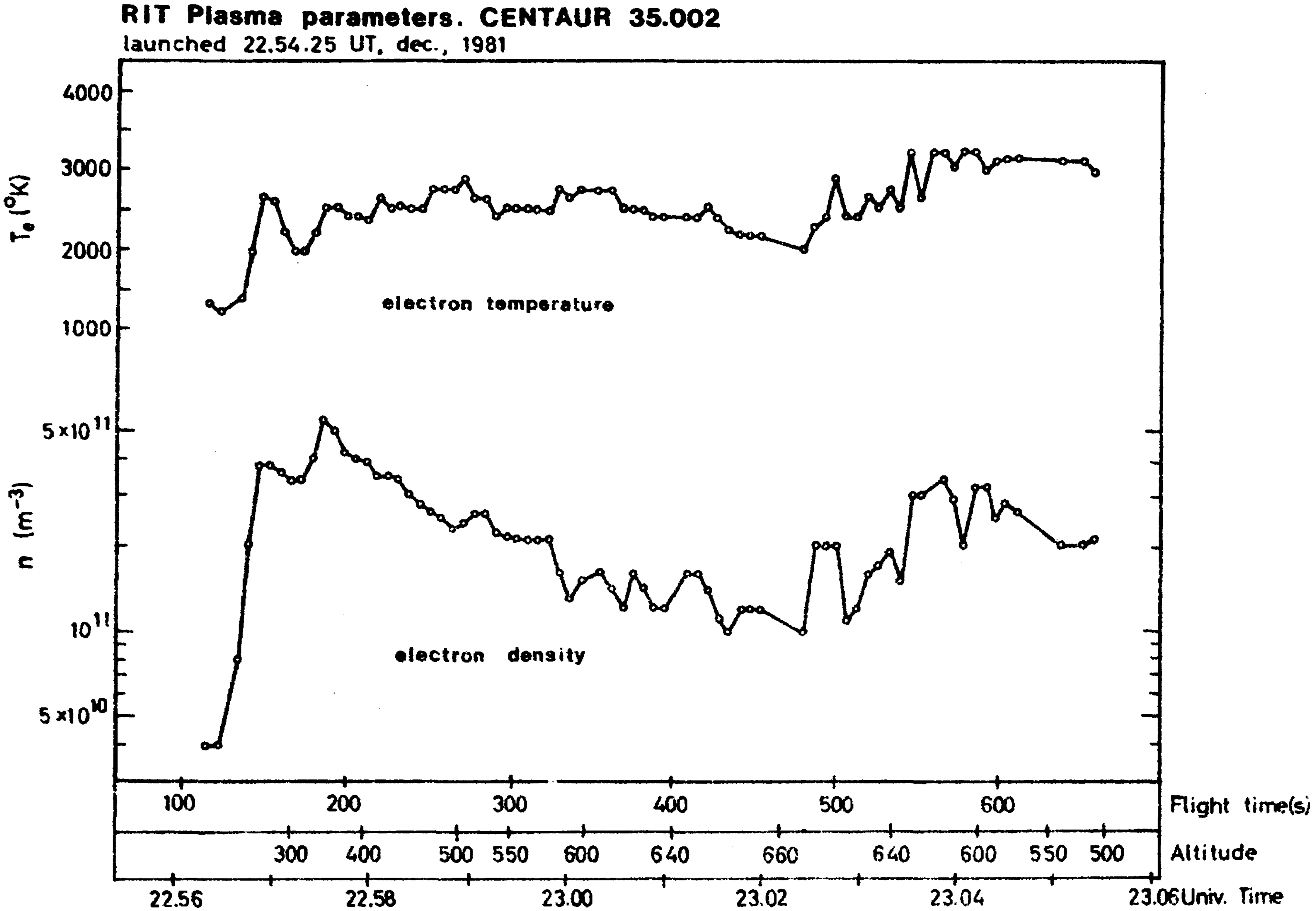

Fig. 7

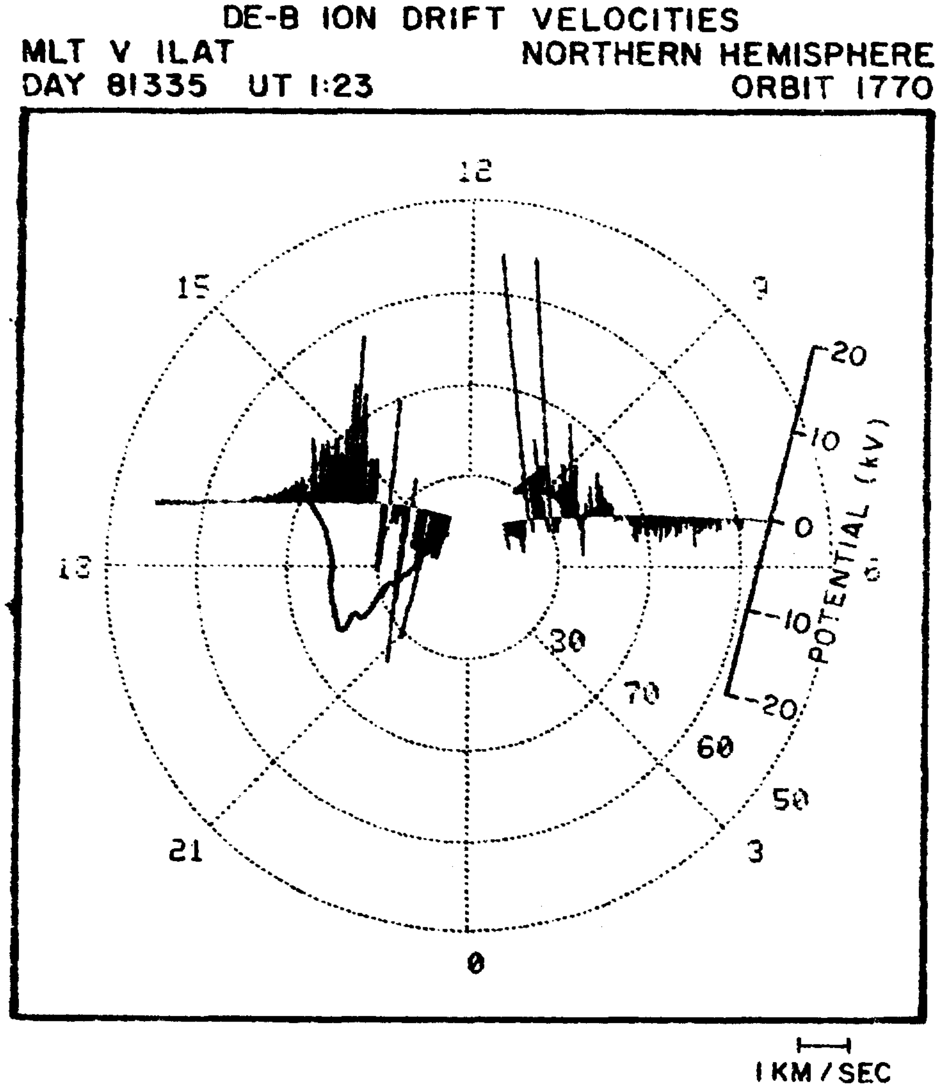
DE-B ION DRIFT VELOCITIES
MLT V ILAT
NORTHERN HEMISPHERE
DAY 81335 UT 1:23
ORBIT 1770
12
15
9
18
6
21
3
0
80
70
60
50
20
10
0
-10
-20
POTENTIAL (kV)
1 KM/SEC

Fig. 8a

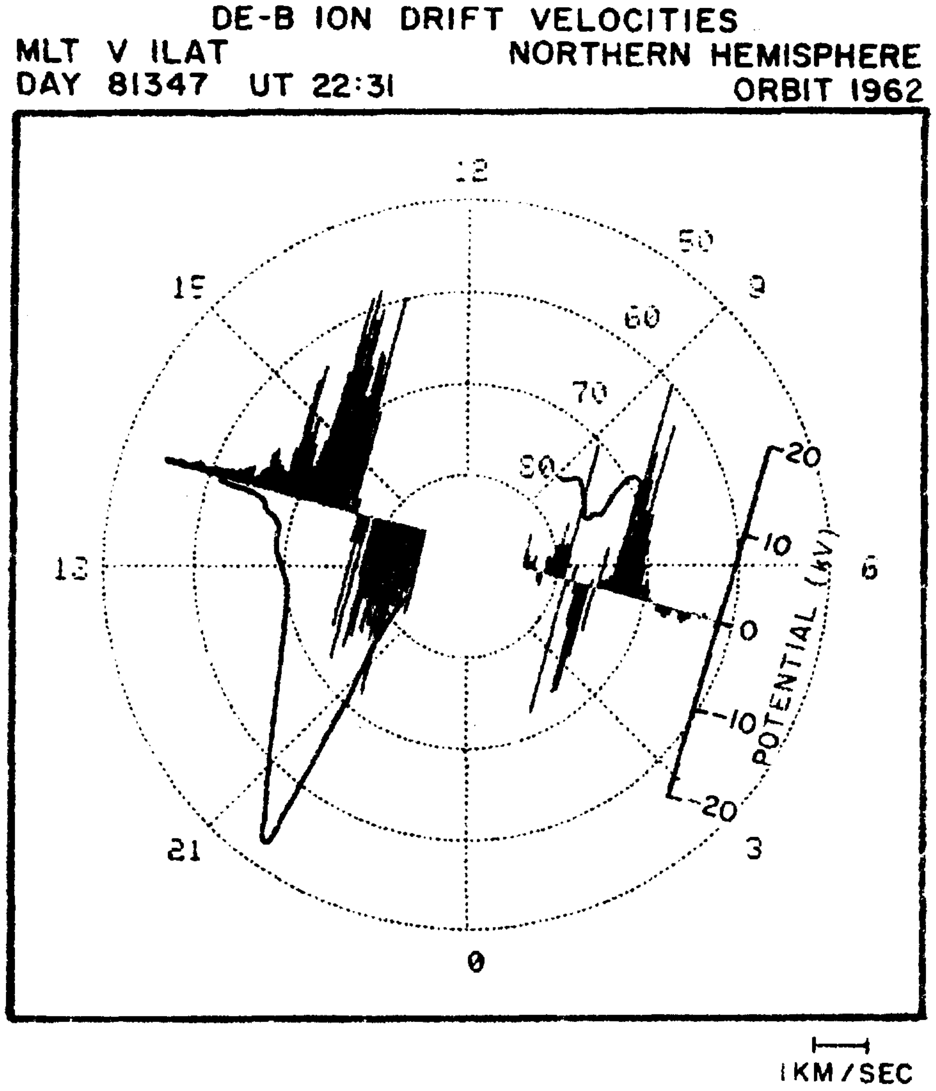
DE-B ION DRIFT VELOCITIES
MLT V ILAT
NORTHERN HEMISPHERE
DAY 81347 UT 22:31
ORBIT 1962
12
15
9
18
6
21
3
0
50
60
70
80
20
10
0
-10
-20
POTENTIAL (kV)
1 KM/SEC

Fig. 8b

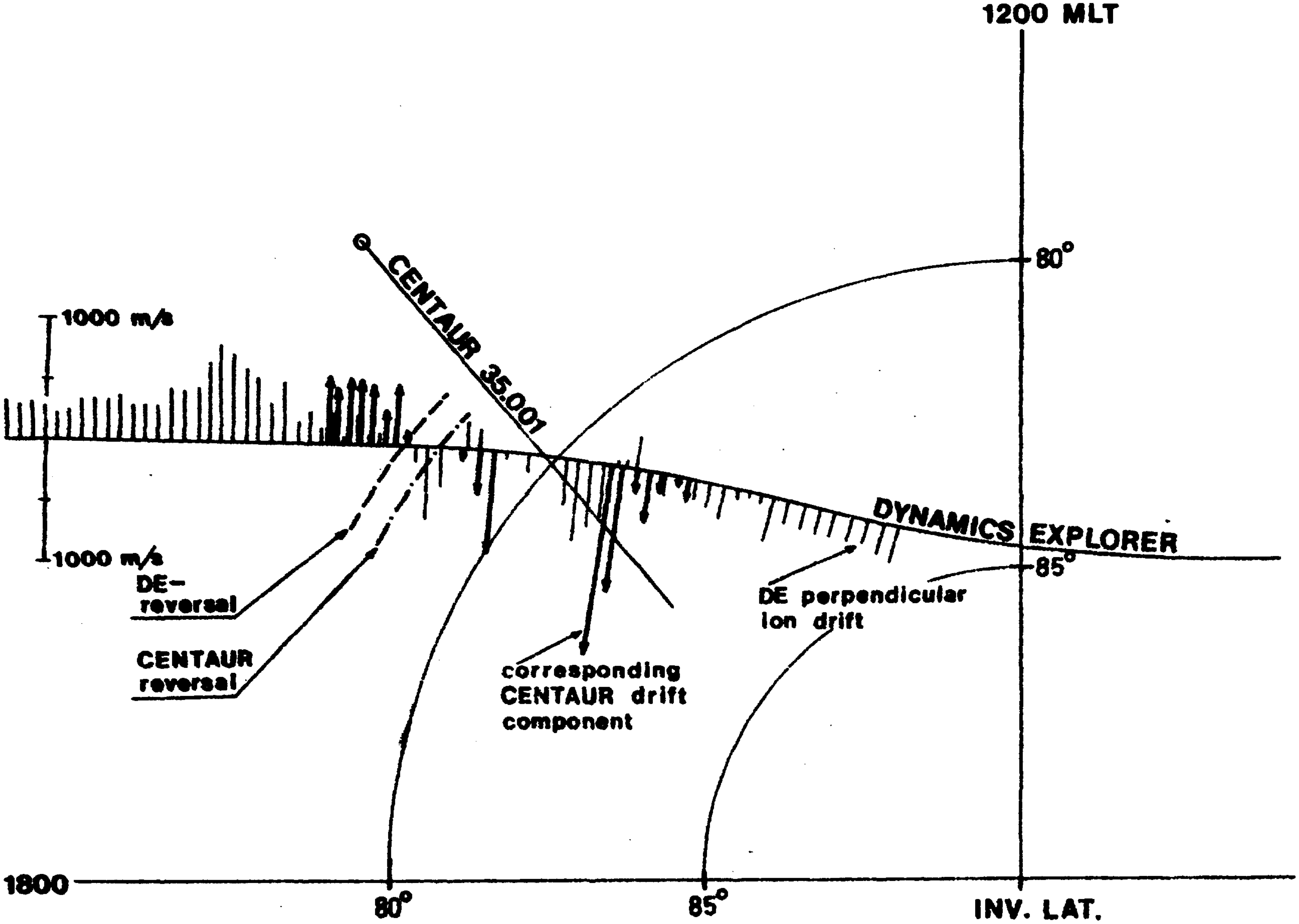
1200 MLT
80°
85°
1000 m/s
1000 m/s
CENTAUR 35.001
DYNAMICS EXPLORER
DE-
reversal
CENTAUR
reversal
corresponding
CENTAUR drift
component
DE perpendicular
ion drift
1800
80°
85°
INV. LAT.

Fig. 9

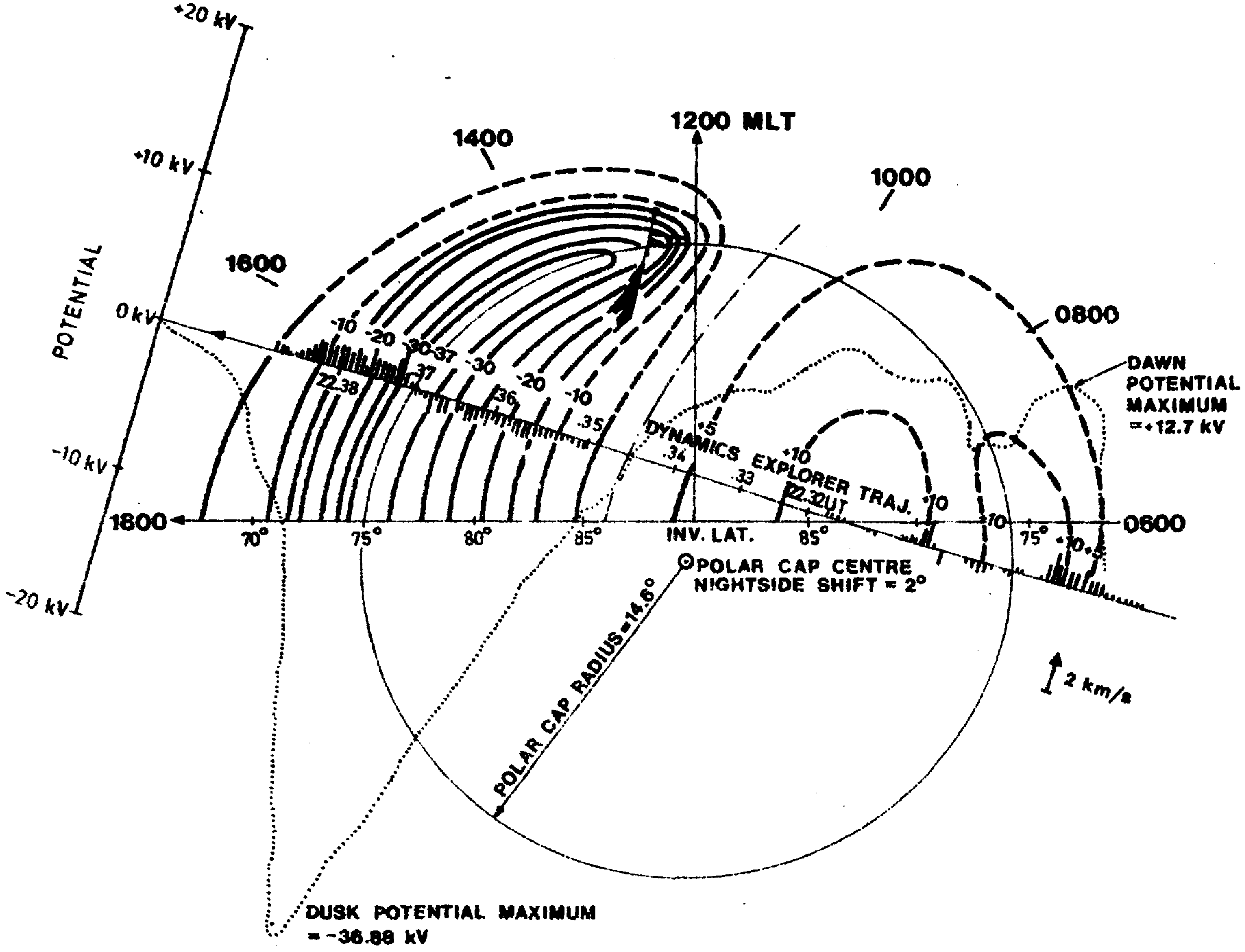
+20 kV
+10 kV
0 kV
-10 kV
-20 kV
POTENTIAL
1200 MLT
1400
1000
1600
0800
1800
0600
70°
75°
80°
85°
INV. LAT.
85°
75°
-10
-20
-30
-37
-30
-20
-10
22.38
.37
.36
.35
.34
.33
22.32UT
+5
+10
+10
+10
+10
+5
DYNAMICS EXPLORER TRAJ.
DAWN POTENTIAL MAXIMUM =+12.7 kV
POLAR CAP CENTRE NIGHTSIDE SHIFT = 2°
POLAR CAP RADIUS =14.6°
2 km/s
DUSK POTENTIAL MAXIMUM = -36.88 kV

Fig. 10a

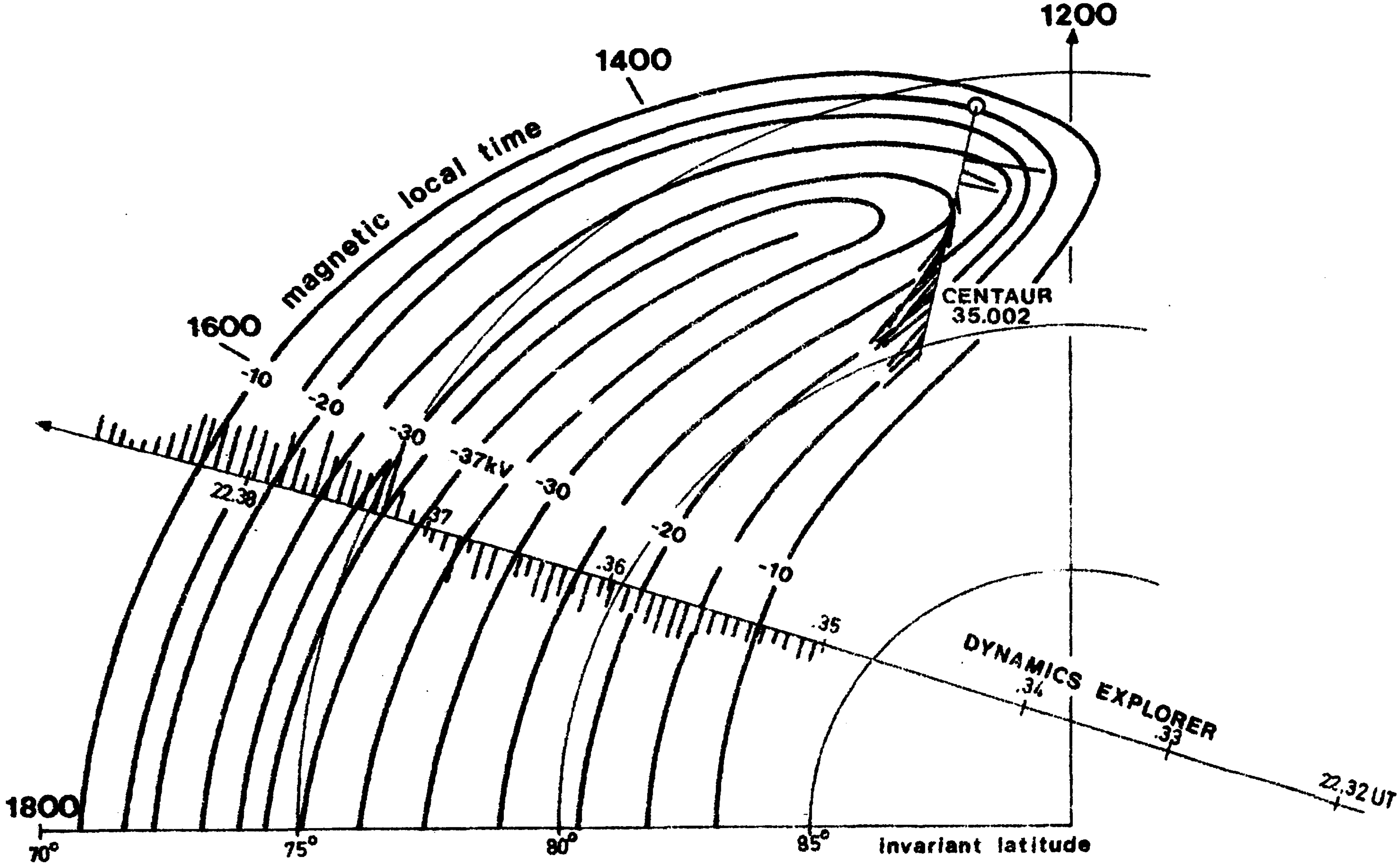

1200
1400
1600
1800
magnetic local time
CENTAUR
35.002
-10
-20
-30
-37kV
-30
-20
-10
22.38
.37
.36
.35
DYNAMICS EXPLORER
.34
.33
22.32 UT
70°
75°
80°
85°
invariant latitude

Fig. 10b

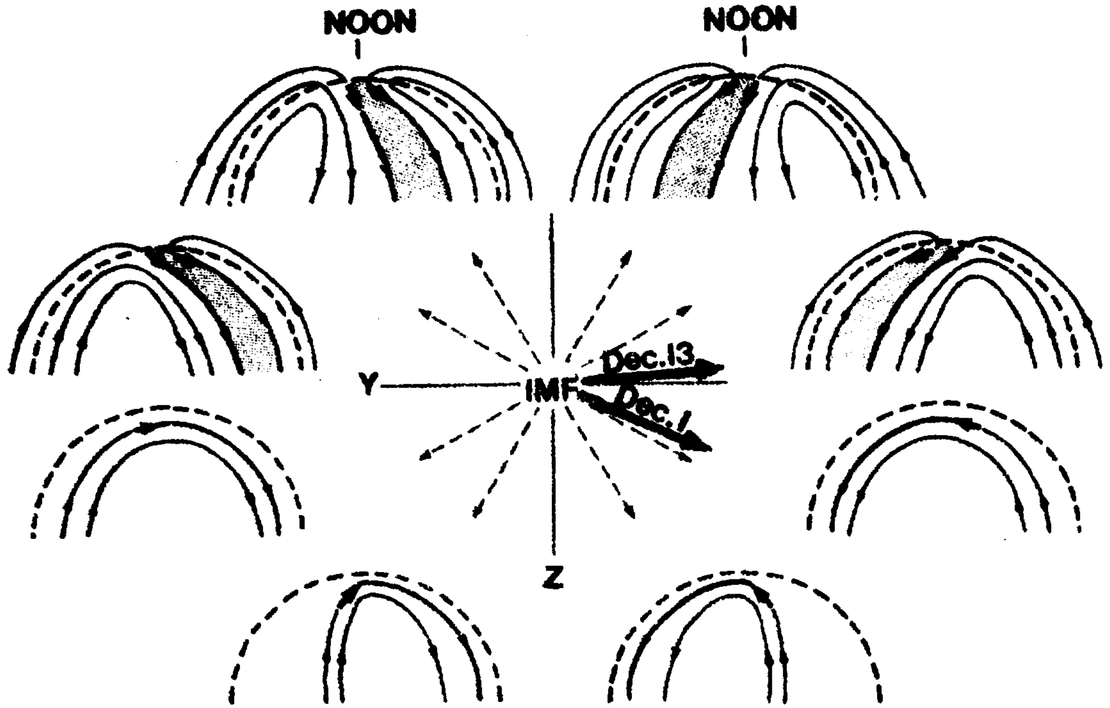

Fig. 11

TRITA-EPP-84-05 ISSN 0348-7539

The Royal Institute of Technology, Department of Plasma Physics,
S-100 44 Stockholm, Sweden

ROCKET AND SATELLITE OBSERVATIONS OF ELECTRIC FIELDS AND ION CONVECTION IN THE DAYSIDE AURORAL IONOSPHERE

G. Marklund and R.A. Heelis

June 1984, 31 pp. incl. illustr., in English

Electric field observations from two high-altitude rocket flights in the polar cusp have been combined with satellite observations of ion drifts to infer details of the electric field and convection pattern of the dayside auroral ionosphere. A region of shear flow reversal can be inferred from the electric field observations on one flight near 15.30 MLT 20 minutes after the Dynamics Explorer 2 satellite crossed through the same region. The drift patterns observed by the two spacecrafts were very similar although shifted by 0.5 degrees, a shift which is expected from the observed change in the interplanetary magnetic field (IMF) B_z component during this time. A region of rotational flow reversal was covered by the other flight shortly after magnetic noon, at the same time the DE-2 satellite travelled along roughly the dawn-dusk meridian. By joining points of equal potential, integrated from the two datasets and assuming the reversal boundary to be an equipotential, the instantaneous convection pattern could be drawn showing crescent-shaped convection contours in the dusk cell and more circular shaped contours in the dawn cell. In order to reproduce this pattern using the convection model recently proposed by Heelis *et al*. (1982) it was found necessary to introduce a local-time dependence of the decay of the electric field with distance from the reversal boundary. Moreover this pattern is shown to be qualitatively in agreement with the predictions of a geometrical model by Crooker (1979) when the IMF is oriented towards dawn. The same characteristic patterns but with the dusk and dawn cells reversed, as presented in a recent radar-satellite study for the IMF oriented towards dusk

Keywords: Convection pattern, Electric fields, Polar cusp, Rotational reversal, Shear reversal.